EXPERIENCE AND DEVELOPMENTS WITH THE LAYER CLOUD AND BOUNDARY LAYER MIXING SCHEMES IN THE UK METEOROLOGICAL OFFICE UNIFIED MODEL

R N B Smith
Meteorological Office
Bracknell
Berkshire, UK

1. Introduction

The UK Meterorological Office uses a unified model for NWP and climate simulation and prediction. Three NWP configurations are run operationally: a global model (GM) for forecasts out to 5 days, a limited area model (LAM) covering the North Atlantic and Europe with twice the horizontal resolution of the global model for more detailed forecasts out to 36 hours and a mesoscale model (MM) covering Britain, Ireland and surrounding areas with approximately 16 km resolution for short range forecasting of the detailed weather over the UK. Both the GM and the LAM have 19 levels but the MM has 30 levels giving better vertical resolution mainly in the boundary layer. A global version with 2.5° x 3.75° horizontal resolution and 19 levels is used for climate prediction and research.

Whenever possible the same dynamical schemes and physical parametrizations are used in each configuration of the model. This policy facilitates the fastest possible progress in improving the model. Thus the optimisation of the AGCM's climatology should also help reduce the systematic errors in the global forecasts and the regular validation of the mesoscale model's forecasts of cloud and precipitation should help improve their simulation in the AGCM. So far there have been no scientific reasons for divergences in the formulations.

The unified model's layer cloud and boundary layer mixing schemes were initially those of Smith (1990). This workshop contribution describes some of the recent developments to these schemes aimed at improving the performance of the unified model (UM). The global models, in climate or NWP modes, have suffered from a cool bias in the troposphere and also deficiencies in their simulation of low cloud and planetary albedo. The latter error leads to the need for large "flux corrections" when the AGCM is coupled to an ocean model because the low cloud affects the net surface radiative flux. Initial tests with the mesoscale model before operational acceptance also showed problems with low cloud and shower prediction.

Two developments are described here:
(a) changes to the layer cloud prediction scheme and to the parameters in the large scale precipitation scheme;
(b) a non-local mixing scheme for the turbulent transport of heat and moisture within unstable boundary layers.
These will now be presented in turn with illustrations of their impact on model performance.

2.(i) Changes to the prognostic cloud water scheme

The prognostic variables which are advected and also transported by the boundary layer turbulent mixing scheme are the liquid/ice water temperature, T_L, and the total water specific humidity, q_w, defined respectively by

$$T_L = T - \frac{L_c}{c_p} q_{cL} - \frac{(L_c + L_F)}{c_p} q_{cF} \tag{2.1}$$

$$q_w = q + q_{cL} + q_{cF} \tag{2.2}$$

where q_{cL} is the specific cloud water and q_{cF} is the specific frozen cloud water.

The cloud scheme partitions the total water into its three components. This is done instantaneously, i.e. there are no rate equations or timesteps involved. The scheme takes the place of the instantaneous removal of supersatuation in models which do not predict cloud water. However, in this scheme cloud is allowed to form before the gridbox becomes saturated. The scheme does this through the assumption that T_L and q_w fluctuate about their predicted gridbox mean values. The quantity required to calculate the cloud amount and water content is the excess of the local total water over the local saturated specific humidity,

$$Q_S = q_w - q_{SAT}(T, p) \tag{2.3}$$

If $Q_S > 0$ cloud exists and the local cloud water is $q_c = Q_S$. Thus when $Q_S > 0$, (2.3) can be rewritten in terms of the "cloud conserved" variables q_w and T_L as

$$Q_S = a_L (q_w - Q_{SAT}(T_L, p)) \tag{2.4}$$

where a_L can be approximated by

$$a_L = \frac{1}{\left(1 + \frac{L\alpha_L}{c_p}\right)} \tag{2.5}$$

$$\alpha_L = \frac{\partial q_{SAT}}{\partial T} \qquad \text{evaluated at } T = T_L \tag{2.6}$$

If $Q_S \leq 0$ there is no cloud and the local cloud water $q_c = 0$, so $T = T_L$ and

$$Q_S = q_w - Q_{SAT}(T_L, p) \tag{2.7}$$

Summarising:

if $q_w > q_{SAT}(T_L,p)$ then $q_c = Q_S = a_L(q_w - q_{SAT}(T_L,p)) > 0$

if $q_w \leq q_{SAT}(T_L,p)$ then $q_c = 0$ and $Q_S = q_w - q_{SAT}(T_L,p) \leq 0$

or in terms of T,

if $q_w > q_{SAT}(T,p)$ then $q_c = Q_S = q_w - q_{SAT}(T,p) > 0$

if $q_w \leq q_{SAT}(T,p)$ then $q_c = 0$ and $Q_S = q_w - q_{SAT}(T,p) \leq 0$

Q_S is now written as a sum of a gridbox mean and a fluctuating part; this can be done in two ways depending on whether T_L or T is chosen as the dependent variable:

T_L-scheme

$$Q_S=\overline{Q_{SL}}+s_L \qquad when \qquad s_L>-\overline{Q_{SL}} \tag{2.8L}$$

$$Q_S=\frac{(\overline{Q_{SL}}+s_L)}{a_L} \qquad when \qquad s_L\leq-\overline{Q_{SL}}$$

where

$$\overline{Q_{SL}}=a_L(\overline{q_w}-q_{SAT}(\overline{T_L},p)) \tag{2.9L}$$

$$s_L=a_L(q_w'-\alpha_L T_L') \tag{2.10L}$$

T-scheme

$$Q_S=\overline{Q_S}+s \tag{2.8}$$

where

$$\overline{Q_S}=\overline{q_w}-q_{SAT}(\overline{T},p) \tag{2.9}$$

$$s=q_w'-\alpha T' \tag{2.10}$$

If the fluctuating quantity s_L or s has a probability distribution function (p.d.f.) G then the gridbox mean cloud fraction, C, and specific cloud water content, q_c, are given by

$$C=\int_{-\overline{Q_{SL}}}^{\infty} G(s_L)\,ds_L \tag{2.11L}$$

$$\overline{q_c}=\int_{-\overline{Q_{SL}}}^{\infty}(\overline{Q_{SL}}+s_L)\,G(s_L)\,ds_L \tag{2.12L}$$

for the T_L-scheme or

$$C=\int_{-\overline{Q_S}}^{\infty} G(s)\,ds \tag{2.11}$$

$$\overline{q_c}=\int_{-\overline{Q_S}}^{\infty}(\overline{Q_S}+s)\,G(s)\,ds \tag{2.12}$$

for the T-scheme. (Note that since s_L and s are different quantities their p.d.f.'s need not be the same.)

Two simple p.d.f.'s have been tried, the so called "top-hat" and "triangular" distributions (see Figure 1). Whichever shape p.d.f. is chosen, the width or standard deviation has to be parametrized. Smith (1990) specified

$$A\sigma_{SL}=(1-RH_c)\,a_L q_{SAT}(T_L,p) \tag{2.13L}$$

in terms of the cloud conserved variable T_L. (A is a constant depending only on the shape of the p.d.f.) This is an uncertain part of the scheme; the form (2.13L) is chosen to allow the specification of a critical relative humidity, RH_C. For the scheme using T the following parametrization has this property

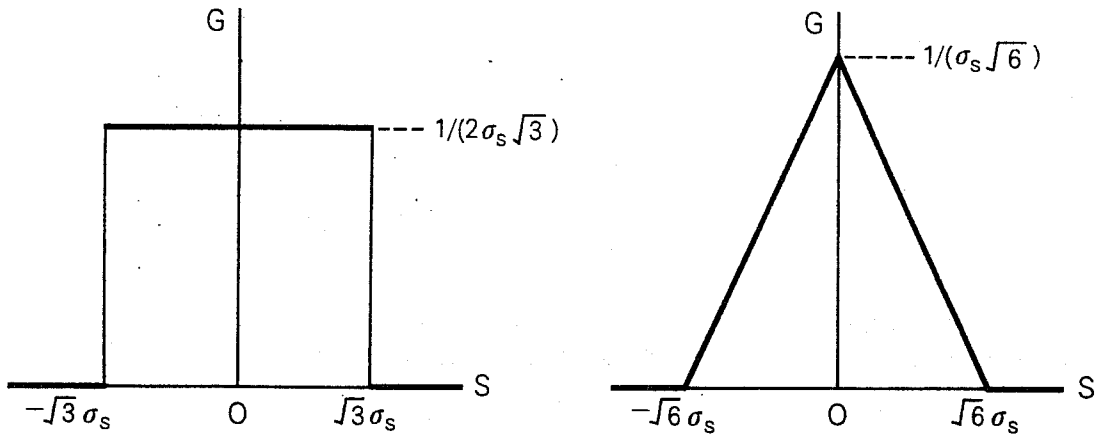

Symmetric 'top-hat' p.d.f. with standard deviation σ_s

Symmetric 'triangular' p.d.f. with standard deviation σ_s

Figure 1. Two simple p.d.f.'s for the cloud ensemble model

$$A\sigma_S = (1-RH_c)\, q_{SAT}(T,p) \tag{2.13}$$

Note that the scheme using T rather than T_L is not as easily used since T is not known until the cloud and hence the latent heating have been calculated. However, with some iteration it can be used as an alternative to the original T_L-scheme.

The unified model calculates cloud radiative properties from the predicted cloud water (Ingram, 1993), so any change to the cloud water sceme may be expected to have an impact on the simulated radiative balance. Figure 6(a) shows the error in the planetary albedo for northern summer (June, July, August) in the climate version of the unified model before any change to the layer cloud and large-scale precipitation schemes (i.e. with the T_L-scheme and triangular p.d.f. and precipitation parameters as given in Smith (1990)). Errors are calculated by subtracting ERBE data. There is obviously excessive albedo in the northern Pacific and Atlantic oceans and not enough boundary layer stratocumulus over the oceans off S.W. Africa, S. America and California.

Figure 2 shows the effect on the model's cloud simulation of changing the shape of the p.d.f. G from "top-hat" to "triangular". (Both experiments used the T-scheme and are JJA means.) The shaded areas indicate where the top-hat distribution gives more cloud. It can be seen that this is mainly in the tropical and subtropical boundary layer. The effect is not very great but marginally benefits the simulated albedo (not shown).

Figure 3 shows the effect of changing from the T-scheme to the T_L-scheme. Exactly the same critical relative humidities were used and both experiments used the triangular p.d.f. Again the results shown are for northern summer using the climate model. The impact of this change is greatest in the midlatitude lower troposphere where the T-scheme gives much less cloud. This is a desirable impact given the overestimate of midlatitude albedo shown in Figure 6(a). It is not yet clear why this change should reduce the cloud amount so much. A plausible hypothesis runs as follows. Evaluating the integrals (2.11(L)) and (2.12(L)) gives the cloud fraction and the *normalised* cloud water content as functions of a normalised "total water relative humidity", r_N:

$$C = f_c(r_N) \tag{2.14}$$

$$\frac{\overline{q_c}}{A\sigma_{S(L)}} = f_q(r_N) \tag{2.15}$$

where the functions f_c and f_q depend only on the shape of the p.d.f. and

$$r_N = \frac{\left(\frac{q_w}{q_{SAT}(T_L,p)} - 1\right)}{(1-RH_c)} \tag{2.16L}$$

for the scheme based on T_L and

$$r_N = \frac{\left(\frac{q_w}{q_{SAT}(T,p)} - 1\right)}{(1-RH_c)} \tag{2.16}$$

for the scheme based on T. The definition of r_N differs in the two schemes but the major difference comes through the standard deviation factor in equation (2.15) for the cloud water. The standard deviation given by (2.13) is larger than than that given by (2.13L)

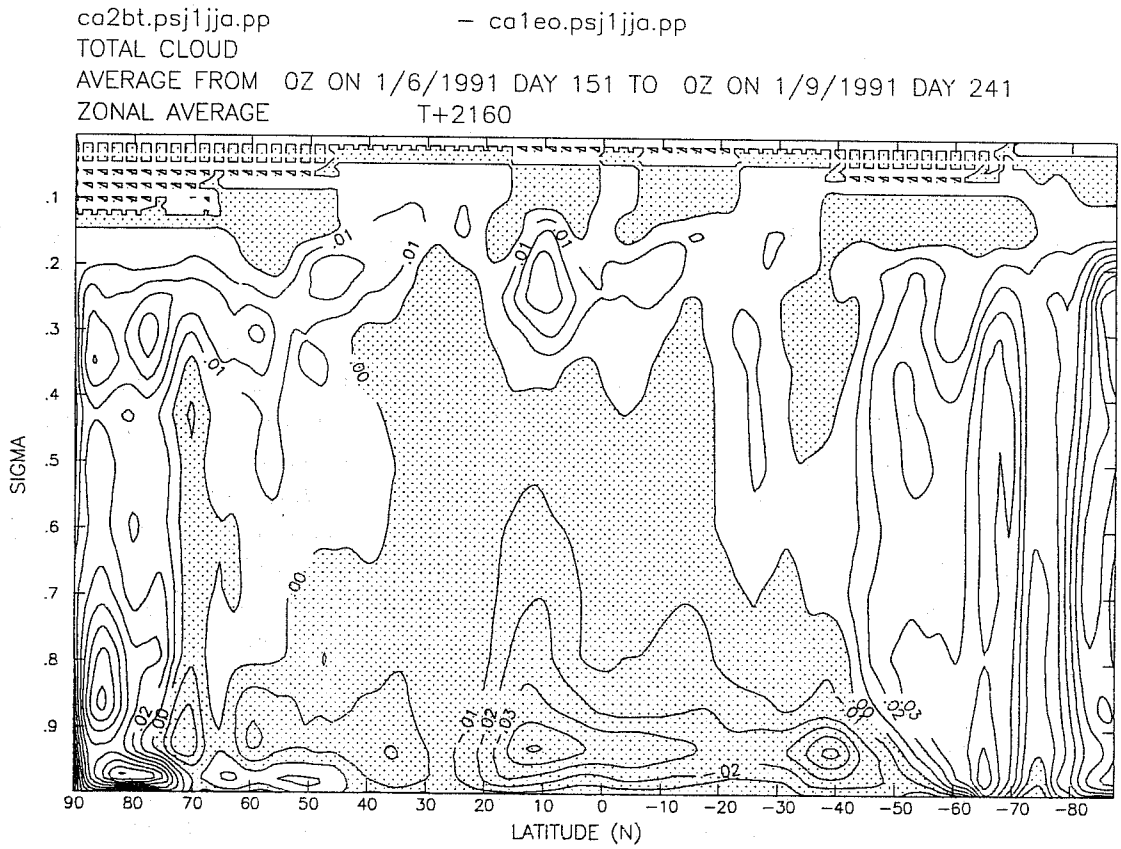

Figure 2. Zonal mean cloud difference of June, July, August means from the climate model: (triangular p.d.f., T-scheme) - (top-hat p.d.f., T-scheme). Contours every 0.01, shaded where negative.

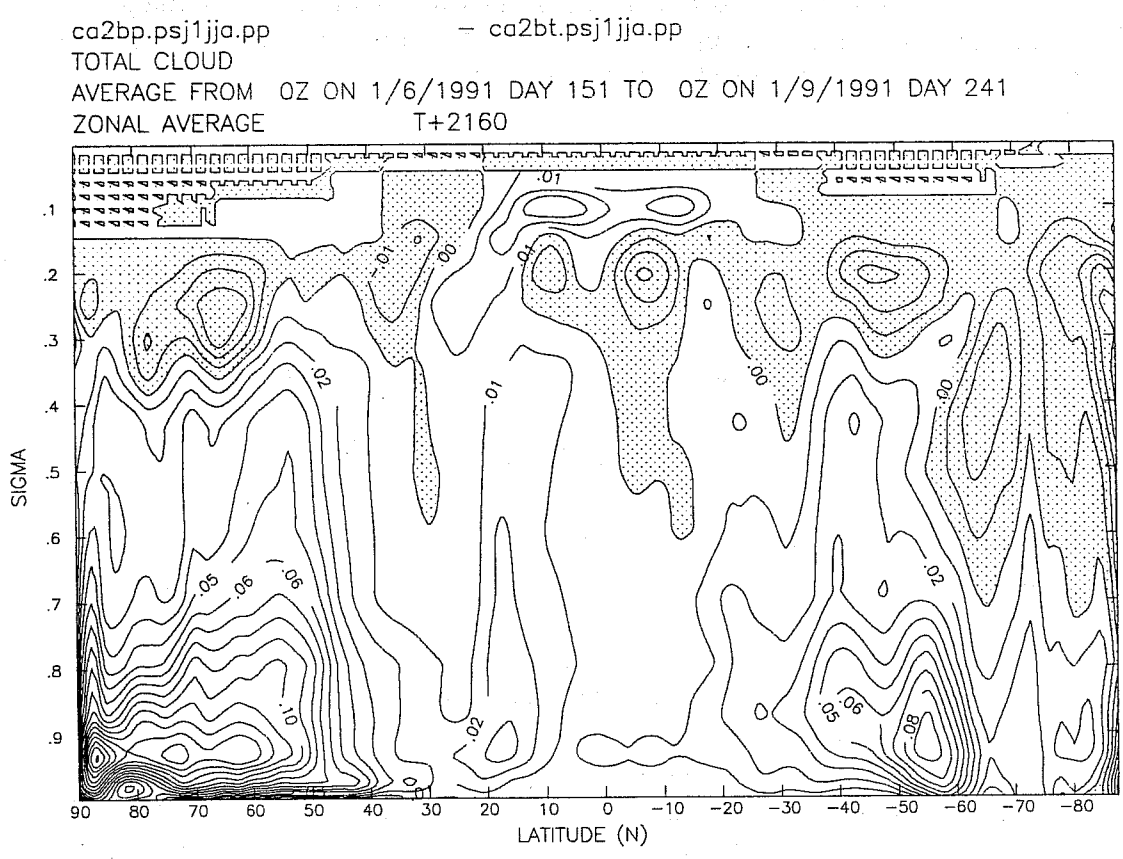

Figure 3. As Figure 2 but showing the difference (triangular p.d.f., T_L-scheme) - (triangular p.d.f., T-scheme).

(a)

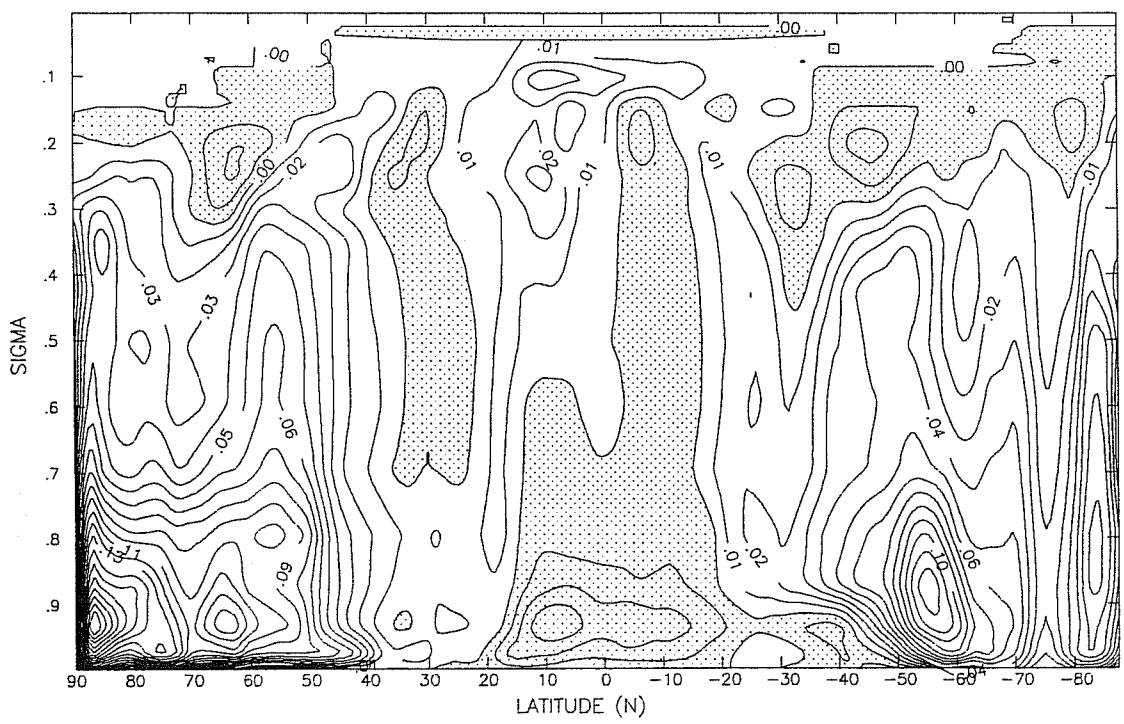

(b)

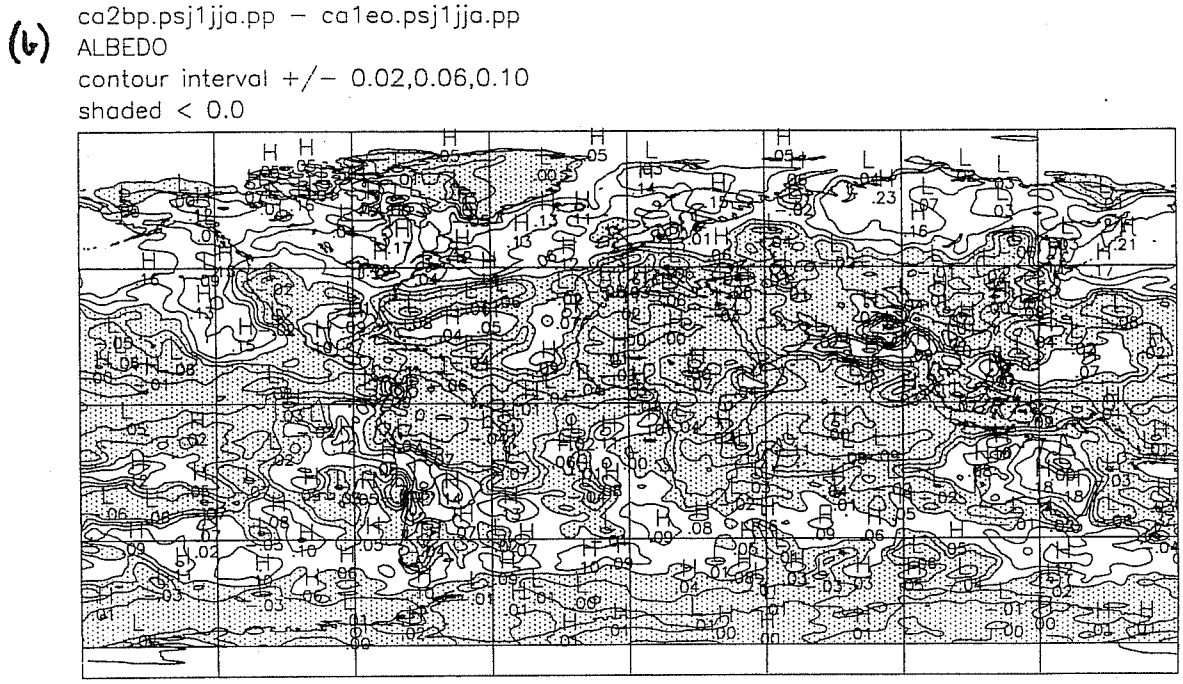

Figure 4. (a) Zonal mean cloud difference of June, July, August means from the climate model: (triangular p.d.f., T_L-scheme) - (top-hat p.d.f., T-scheme). Contours every 0.01, shaded where negative.
(b) Planetary albedo difference for the same period and same experiments as in (a).

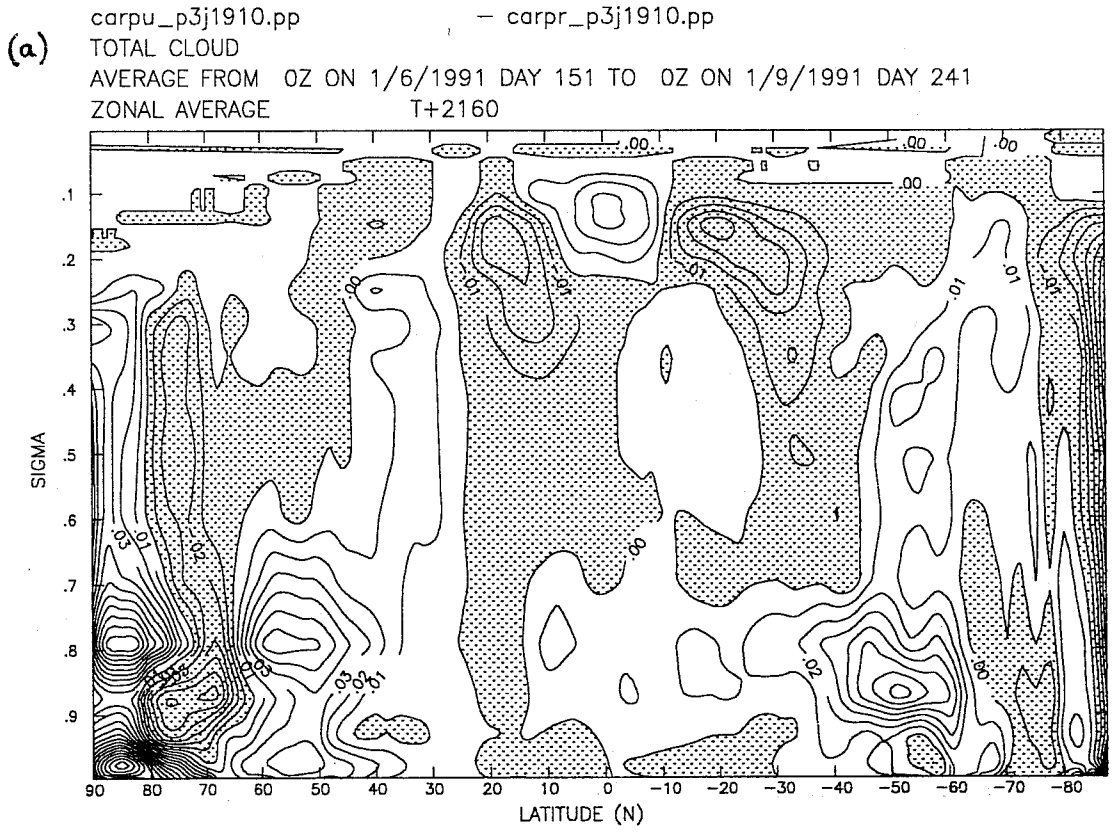

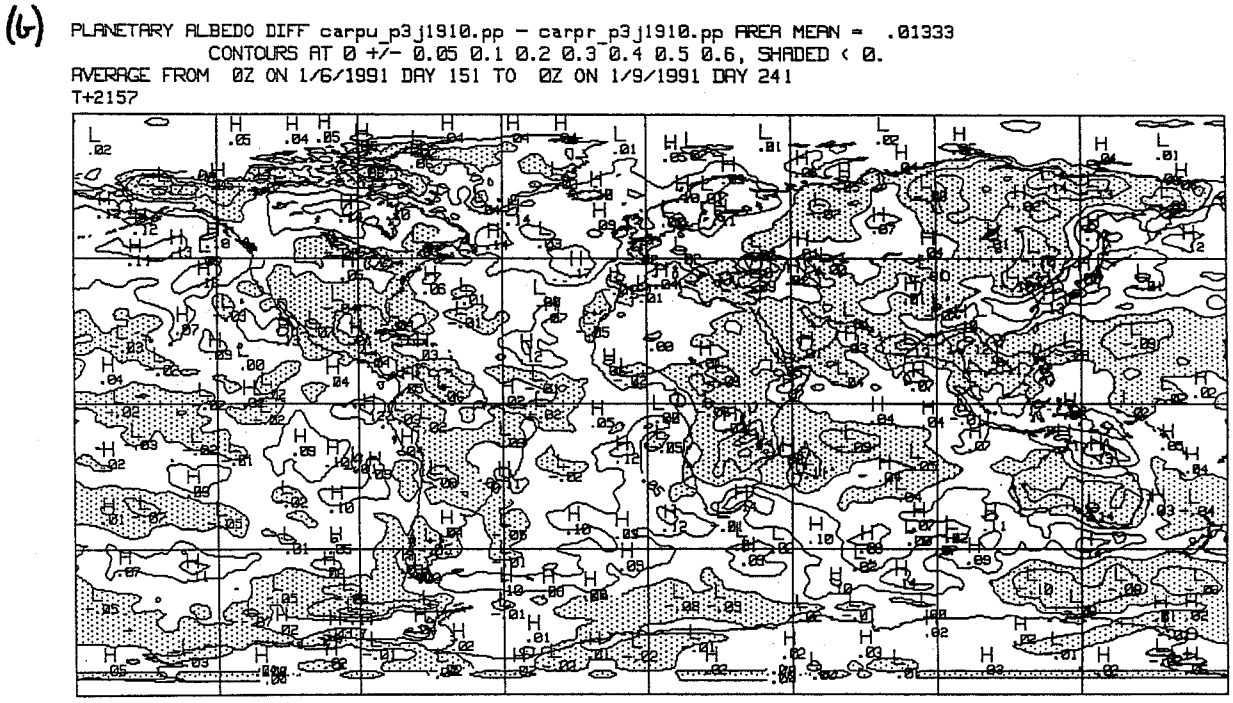

Figure 5. (a) Zonal mean cloud difference of June, July, August means from the climate model:
(Expt. with $c_w = 0.8 \times 10^{-3}$ kg m^{-3}) - (Expt. with $c_w = 0.2 \times 10^{-3}$ kg m^{-3} at sea points)
Contours every 0.01, shaded where negative.
(b) Planetary albedo difference for the same period and same experiments as in (a).

even when identical values of the critical relative humidity are used. This is because $a_L < 1$ and $T_L \leq T$. So for a given cloud amount the T-scheme will give a larger water content. This will allow precipitation to form more easily and hence reduce the cloud amount. Some support for this arguement comes form comparing the total cloud liquid water path through the depth of the atmosphere from simulations using the two schemes (not shown). There is more cloud water when the T-scheme is used even though there is less cloud.

The interaction of this type of cloud scheme with precipitation processes can be criticised. Details of the cloud or precipitation schemes can be changed with initially surprising effects which are difficult to understand. Nevertheless until observed data can give clear guidance on the most appropriate shapes and widths of the p.d.f. for various cloud types we chose the specification which gives best predictions.

Figure 4 shows the effect of combining the change of the p.d.f. from top-hat to triangular and from changing from the T-scheme to the T_L-scheme. The zonal mean cloud amount differences (Figure 4(a)) show that the (T,top-hat)-scheme gives less cloud in the mid-latitudes and more in the lower latitudes, the largest effect being in the boundary layer. The associated change in the planetary albedo is shown in Figure 4(b). The (T,top-hat)-scheme gives lower albedo over mid-latitude oceans and slightly larger subtropical values. Given the large error in the simulated albedo (Figure 6(a)) in the early stages of development of the climate model when the (T_L,triangular)-scheme was used, it was decided to adopt the (T,top-hat)-scheme. Other aspects of the model simulation are little affected by the change.

(ii) The effect of a change to the threshold for efficient rainfall production

The rate of conversion of cloud liquid water to rain is parametrized as

$$\left(\frac{\partial q_L}{\partial t}\right)_{PPN} = -\left[c_t\left\{1-\exp\left[-\left(\frac{\rho q_L/C}{c_w}\right)^2\right]\right\}+c_a P\right]q_L \qquad (2.17)$$

(see Smith,1990). The parameter c_w determines the cloud water content above which conversion to rain becomes efficient. If the in-cloud liquid water content, $\rho q_L/C$, is less than c_w, the production of rain is inhibited. The original value used for c_w was 0.8×10^{-3} kg m^{-3} everywhere. Because air over oceans has less cloud condensation nuclei the drops grow larger and so precipitate more easily. This implies that oceanic clouds can hold less water and so a lower value for c_w is appropriate over sea points. The effect of changing the value of c_w to 0.2×10^{-3} kg m^{-3} at sea points only can be seen in figure 5. The unshaded areas show where the cloud cover (Fig. 5(a)) or albedo (Fig. 5(b)) are lower in the simulation with a lower value for c_w over sea. There is a beneficial impact over mid-latitude oceans.

(iii) Remaining deficiencies in the model's low cloud

The impact on the climate model's simulated June, July, August mean albedo of changing:

(a) the p.d.f. to top-hat,

(b) the dependent variable in the expression for σ_S to T,

(c)the value of c_w at sea points to 0.2×10^{-3},

together can be seen by comparing Figures 6(a) and 6(b). The main errors evident in

(a)

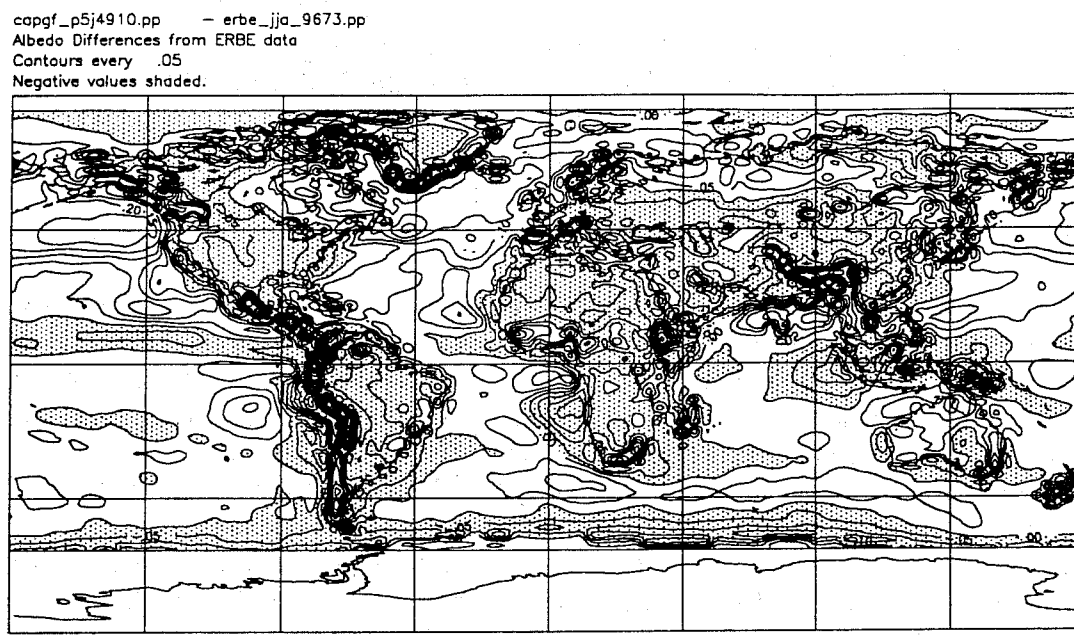

(b)

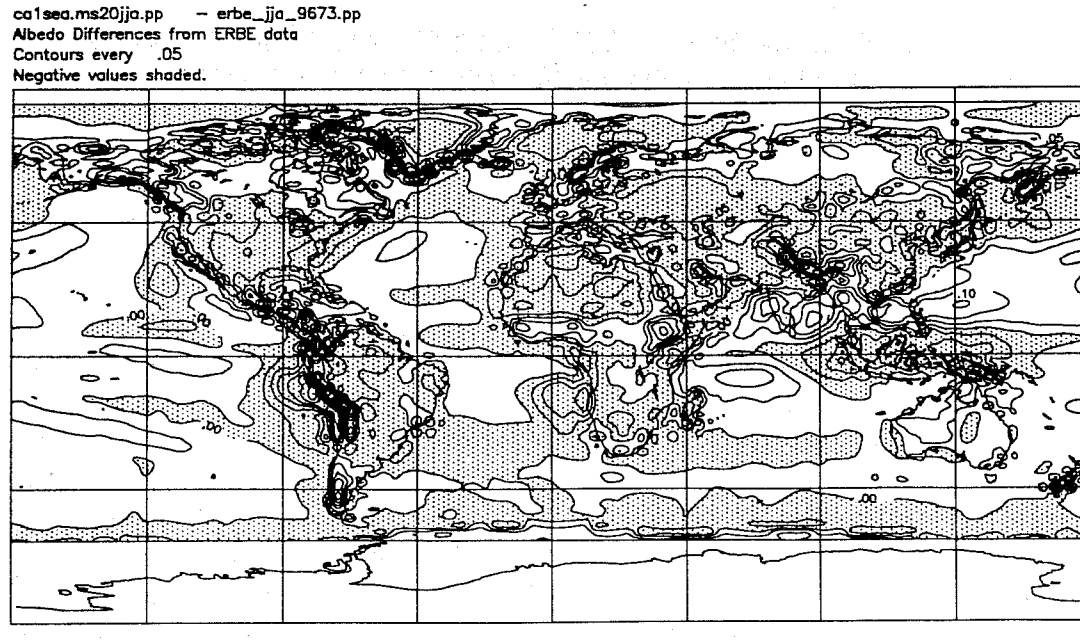

Figure 6. (a) Error in the original climate model's planetary albedo. Model - ERBE data. (b) Same as (a) but after changing to the layer cloud scheme to (top hat, T) and lowering c_w to 0.2×10^{-3} kg m^{-3} at sea points.

Figure 6(a) have already been discussed. Clearly from Figure 6(b) it can be seen that the overestimate of mid-latitude albedo has been alleviated but the stratocumulus off the west coasts of southern Africa, South America and California remains substantially underpredicted.

Figure 7 shows the comparison of the revised model's total cloud liquid water path zonally meaned over sea points for June with SMM/I observations for June 1988 (Greenwald, 1993). The model's cloud water is excessive over mid-latitude oceans in the summer hemisphere. The maps in Figure 8 show that model's liquid water path through the depth of the atmosphere can exceed twice the measured value in regions of the northern Pacific and Atlantic oceans. This is not necessarily caused by deficiencies in the large-scale cloud and precipitation schemes. It is known that the model's mid-latitude troposphere is too moist and cool and this could be a cause of the errors in cloud and cloud water. It is a possibility worth investigating that moisture is not being removed properly from the model atmosphere by subgrid processes like convection.

The lack of oceanic stratocumulus in the subtropics is not uncommon in models with crude vertical resolution in the boundary layer. Future work will assess the impact on stratocumulus simulation of increased vertical resolution and of calculating σ_s in terms of parametrized turbulent fluctuations.

3. (i) A non-local scheme for boundary layer turbulent mixing

The unified model now has two schemes available for calculating the turbulent fluxes and mixing increments in the boundary layer. One is of the standard "local mixing" type, i.e. the flux of a conserved quantity X is parametrized using a first-order closure:

$$F_X = -\rho K_X \frac{\partial X}{\partial z} \tag{3.1}$$

where K_X is the turbulent mixing coefficient for X which is a function of a mixing length, the local wind shear and *local* stability. The rate of change of X due to turbulent mixing is then

$$\left(\frac{\partial X}{\partial t}\right)_{tm} = g\frac{\partial F_X}{\partial p} \tag{3.2}$$

Details can be found in Smith (1990) or Smith (1993).

An alternative scheme allows non-local mixing of heat and moisture in unstable conditions when the boundary layer is more than one model layer deep. This was developed because of the following potential deficiencies of the local mixing scheme:

- in unstable, rapidly mixing regions the fluxes are not observed to be closely related to local gradients - the edies or plumes which are doing the mixing have large vertical extent and correlation;
- forming flux divergences over relatively thin model layers (particularly the lowest model layer) can cause numerical problems when the timestep is large and the turbulent mixing coefficients are large (as they are in unstable boundary layers). An implicit scheme prevents numerical instability but sometimes at the cost of accuracy;
- the local values of stability on which the mixing coefficients depend are partly determined by other parts of the model, particularly the convection scheme. The unified model's convection scheme (Gregory and Rowntree, 1990) tends to overstabilise the boundary layer and hence it can switch off turbulent mixing based entirely on local gradients.

The non-local mixing scheme uniformly distributes the heating and moistening resulting

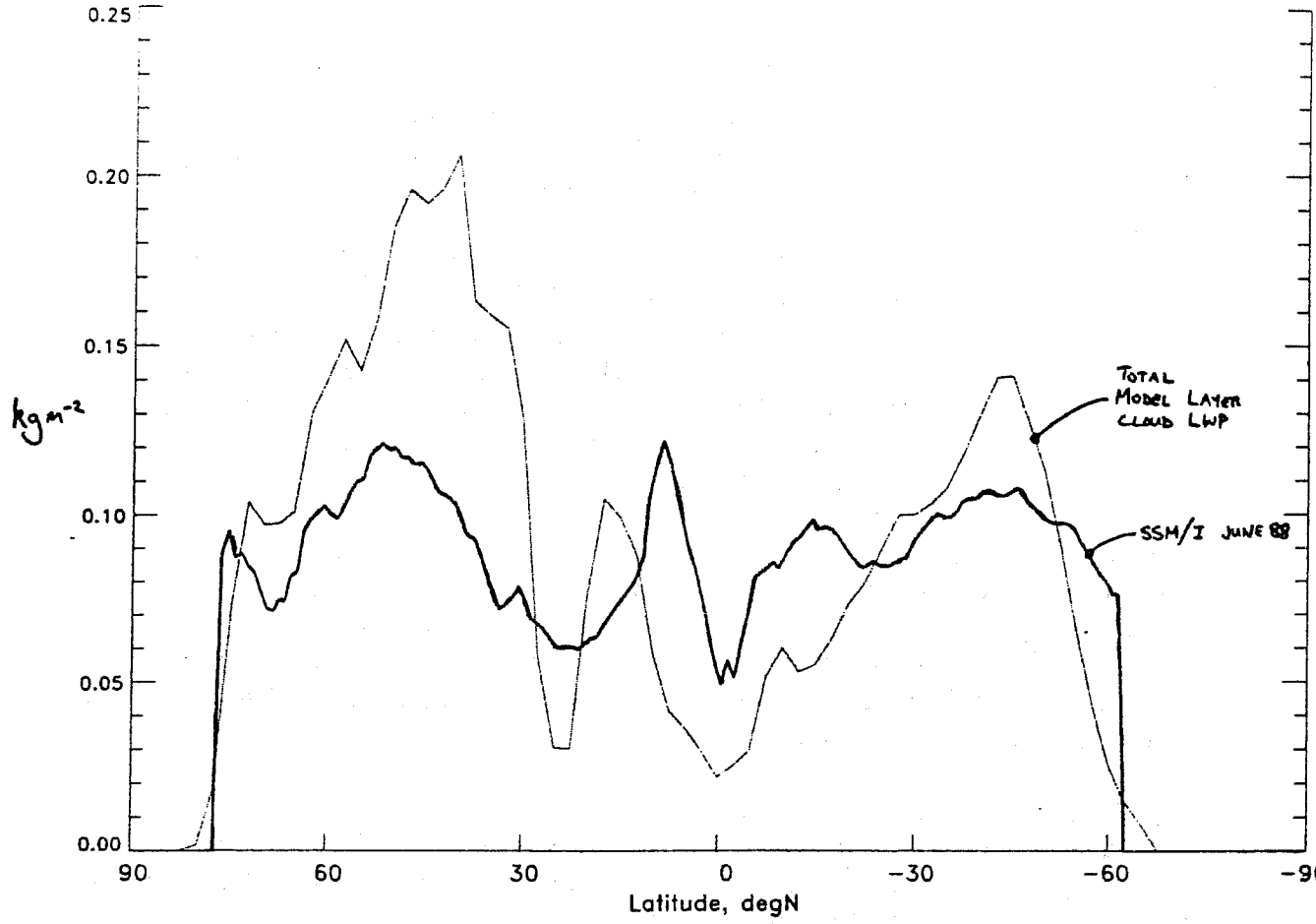

Figure 7. Modelled and observed total liquid cloud water path zonally meaned over sea points. Model is that with (top-hat, T) cloud scheme and $c_w = 0.2 \times 10^{-3}$ kg m^{-3} at sea points. Observed is from SSM/I data.

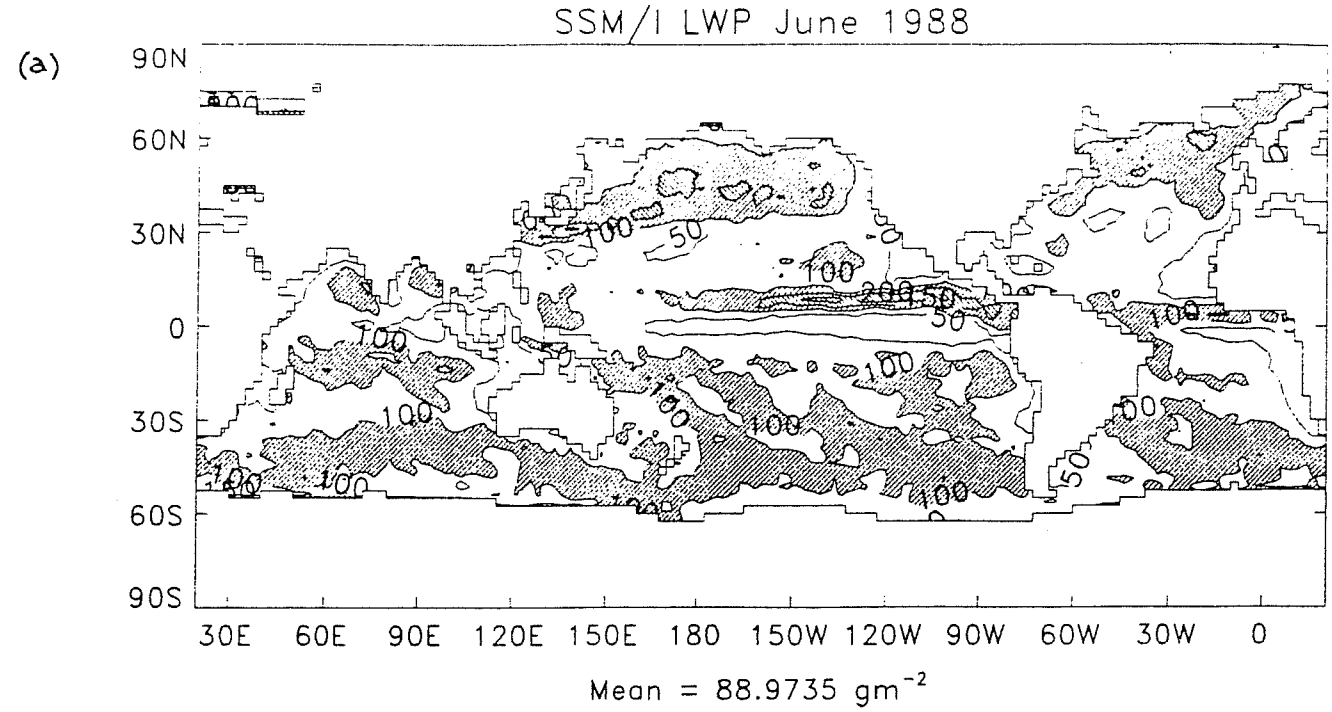

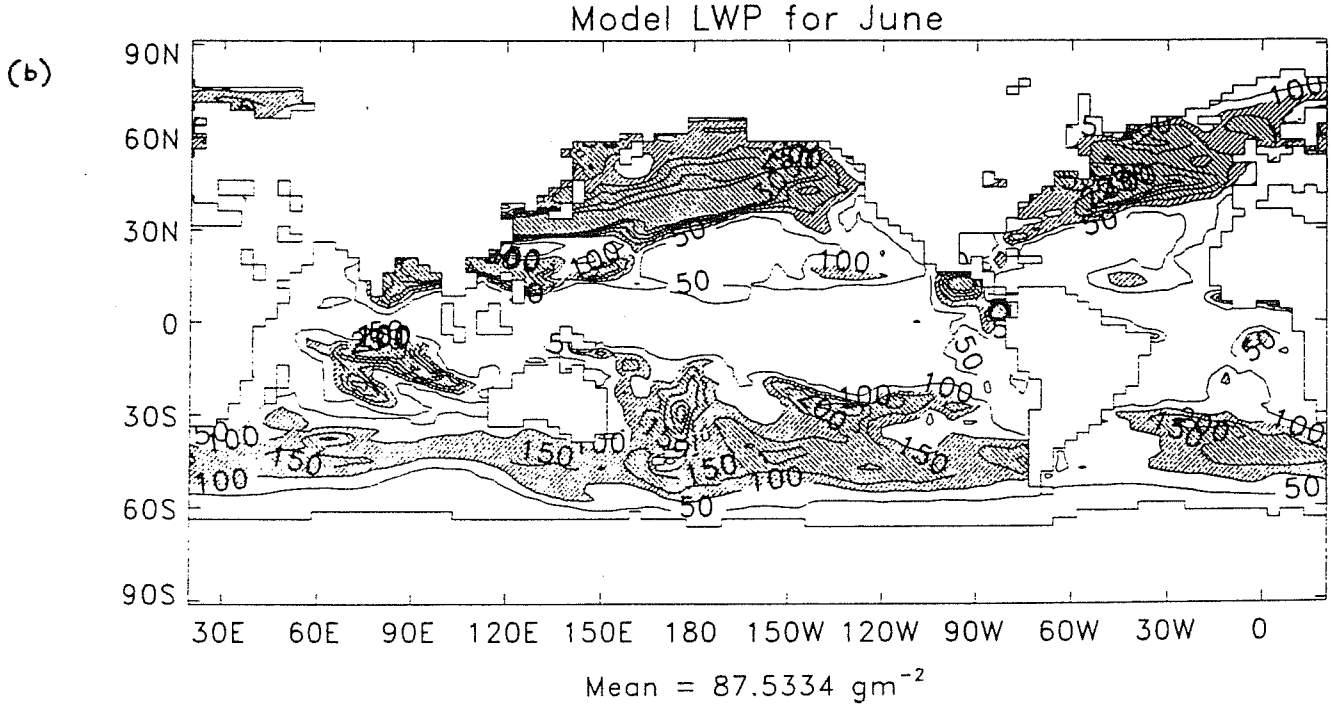

Figure 8. Modelled and observed total liquid cloud water path zonally meaned over sea points. Model and data as in Figure 7. Contours every 50 g m^{-3}.

from the divergence of the fluxes between the surface and the top of the boundary layer. This implies profiles of non-local fluxes $F_X^{(NL)}$ which are linear with resect to pressure in the mixing layer

$$F_X^{(NL)}(p) = \frac{[(p_T - p)\,F_{X(*)} + (p - p_*)\,F_{X(T)}]}{(p_T - p_*)} \tag{3.3}$$

Subscripts * and T denote surface and top of boundary layer values respectively. It is easily seen that inserting the non-local fluxes given by (3.3) into (3.2) gives a uniform increment below the boundary layer top. The surface and top-of-boundary-layer fluxes are calculated exactly as in the local scheme. The number of model layers in the boundary layer is diagnosed from the local Richardson number profile but there is a test to see if it can deepen within the timestep. The uniform increments applied to all the model layers within the mixing layer do not alter the shape of the profiles. This is not very realistic so the scheme also assumes that there is local mixing between adjacent model layers *within* the mixing layer effected by local fluxes given by (3.1). The total flux at a given model layer interface within the mixing layer is therefore the sum of a non-local flux given by (3.3) and a local flux given by (3.1).

The total increment to X in model layer k due to turbulent turbulent mixing is

$$(\delta X_k)_{tm} = (\delta X)_{rm} + (\delta X_k)_{lm} \tag{3.4}$$

where $(\delta X)_{rm}$ is the increment (uniform within the mixing layer) due to non-local "rapid mixing" given by

$$(\delta X)_{rm} = (g\delta t/\Delta p_{rml})\,(F_X(N_{rml}+1/2) - F_{X(*)}) \tag{3.5}$$

where

$$\Delta p_{rml} = \sum_{k=1}^{N_{rml}} \Delta p_k \tag{3.6}$$

and N_{rml} is the diagnosed number of model layers within the mixing layer. $(\delta X_k)_{lm}$ is the local increment give by

$$(\delta X_k)_{lm} = (g\delta t/\Delta p_k)\left(F_X^{(lm)}(k+1/2) - F_X^{(lm)}(k-1/2)\right) \tag{3.7}$$

for $2 \le k \le N_{rml} - 1$,

$$(\delta X_k)_{lm} = (g\delta t/\Delta p_k)\,F_X^{(lm)}(k+1/2) \tag{3.8}$$

for $k = 1$ and

$$(\delta X_k)_{lm} = -(g\delta t/\Delta p_k)\,F_X^{(lm)}(k-1/2) \tag{3.9}$$

for $k = N_{rml}$. The special one-sided flux divergences in (3.8) and (3.9) are required because the surface and top-of-b.l. fluxes are already accounted for in the "rapid mixing" increment given by (3.5). The scheme is set out diagramatically in Figure 9.

The increments are calculated using an implicit numerical scheme. It turns out that the implicit equations for the local and non-local increments decouple so the scheme only has

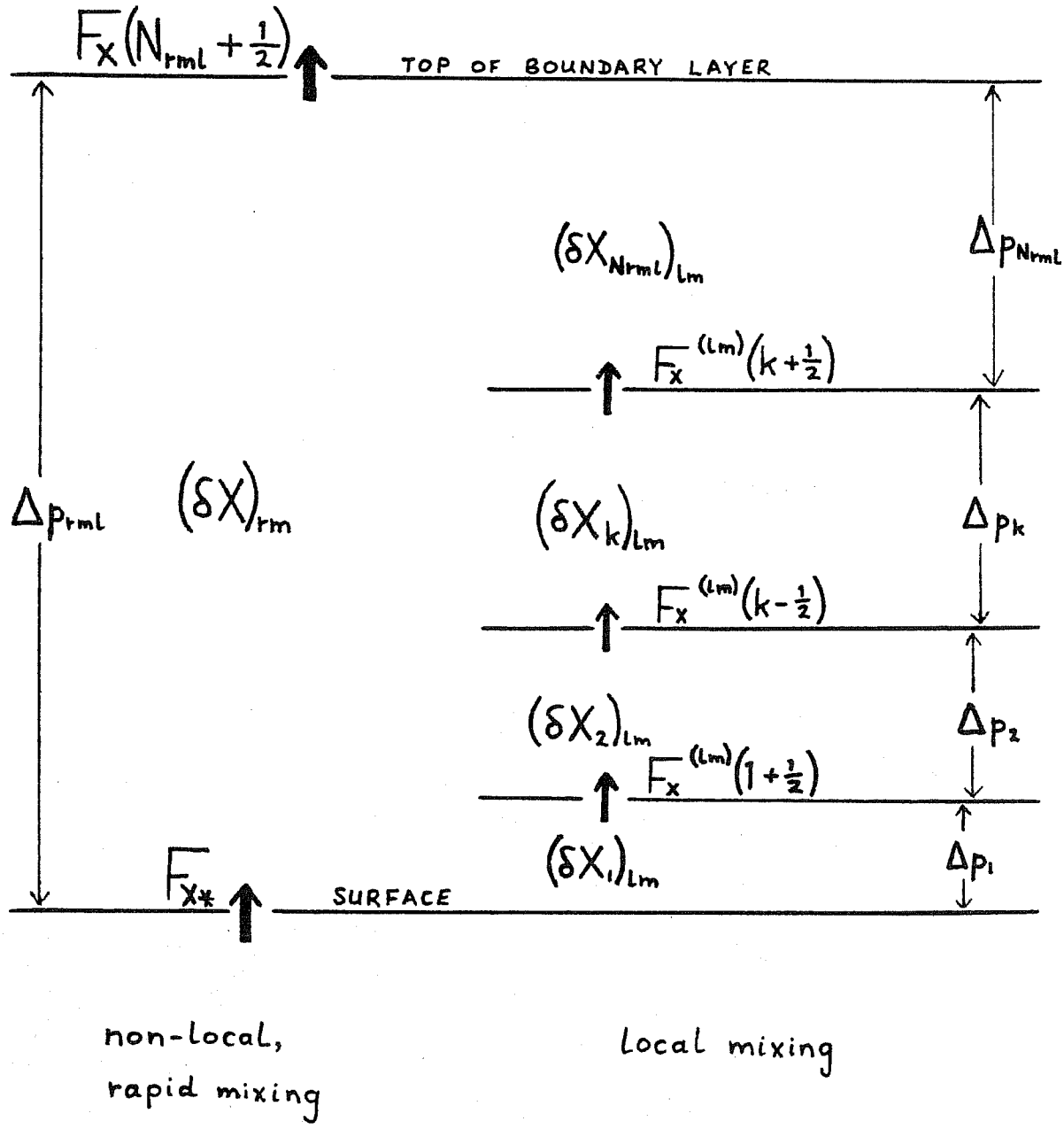

Figure 9. Diagram showing how the rapid and local mixing increments are calculated in the non-local turbulent mixing scheme.

(a)

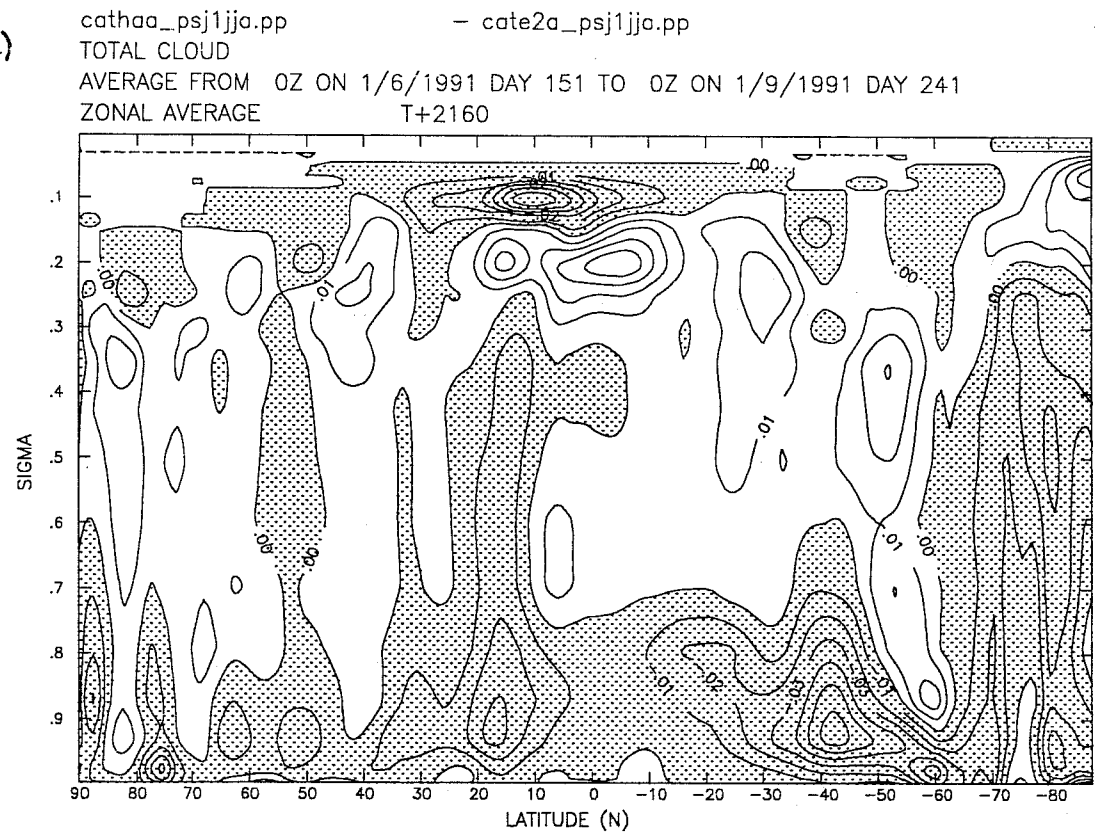

(b)

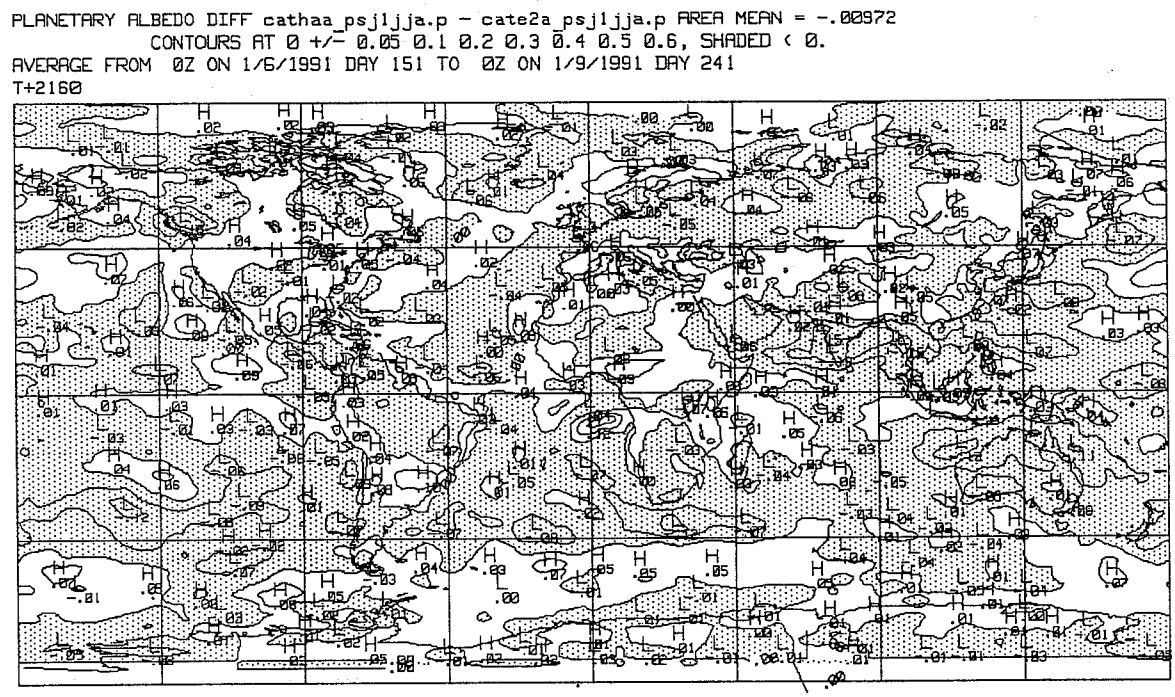

Figure 10. (a) Zonal mean cloud difference of June, July, August means from the climate model: Local mixing scheme - non-local mixing scheme. Contours every 0.01, shaded where negative.
(b) Planetary albedo difference for the same period and experiments as in (a)

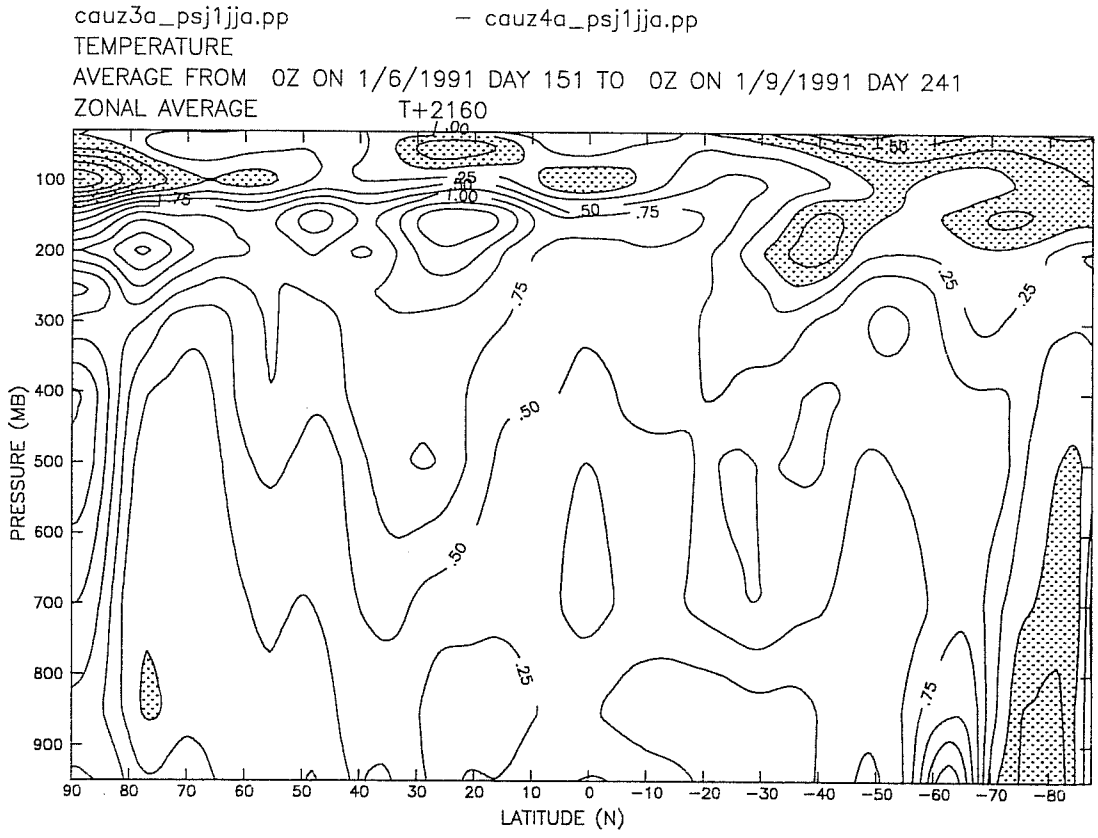

Figure 11. Zonal mean temperature difference of June, July, August means from the climate model: Non-local mixing scheme - local mixing scheme.
Contours every 0.25 K, shaded where negative.

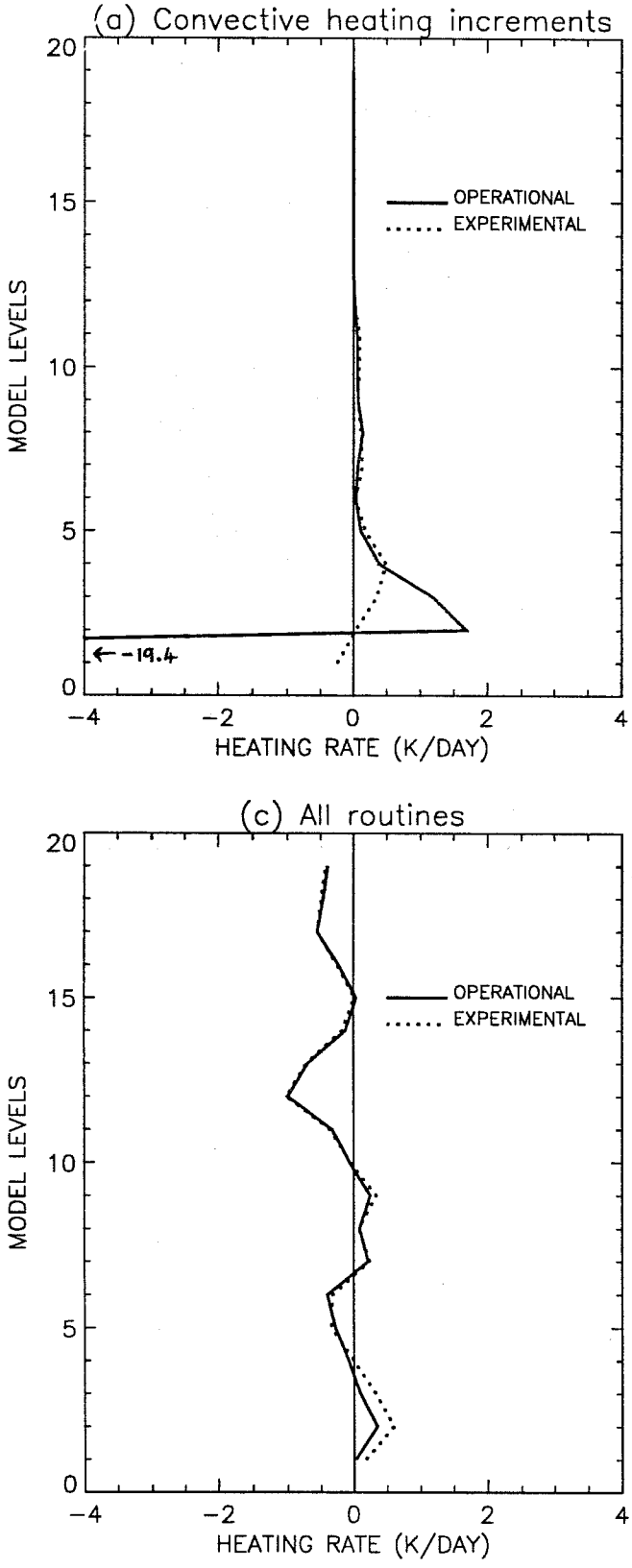

Figure 12. 50°N zonal mean heating rates from the globa NWP model averaged over 1 day (on 20 September 1991). Solid line using local mixing scheme, dotted line using non-local scheme.

to deal with tridiagonal matrices as with the local scheme (details can be found in Smith, 1993).

The non-local scheme can be regarded as a particular example of Stull's (1984) class of "transilient" mixing schemes. Only "large-eddy" mixing across the whole of the boundary layer and small eddies mixing between adjacent model layers are considered rather than a whole spectrum of eddy sizes.

(ii) Impacts of the non-local mixing scheme

Figure 10(a) shows the effect of the alternative turbulent mixing scheme on the zonal mean cloud amount in June, July, August as simulated by the climate version of the model. The shaded areas show where the non-local scheme increases the cloud amounts. The impact is small and mainly in the boundary layer. Figure 10(b) shows that the non-local scheme increases the planetary albedo (shaded areas) mainly over lower latitude oceans. This goes a small way towards correcting the model's bias in these regions. However, the large errors in albedo where the model fails to predict enough oceanic stratocumulus are not substantially corrected. As discussed in Section 2 above, these errors are probably due to a lack of vertical resolution in the boundary layer. It is perhaps not too surprising that the non-local scheme, which is really only a change to the numerical integration scheme, has not on its own corrected the bad stratocumulus simulation.

The non-local scheme goes some way towards correcting another of the model's systematic biases, that of too cool a troposphere. Figure 11 shows the zonal mean temperature difference with the two turbulent mixing schemes. The local scheme is the control in this diagram so the unshaded areas show where the non-local scheme gives a relatively warm simulation, i.e.nearly all the troposphere. However, the model still has a cold bias in the troposphere even with the non-local scheme.

It is thought that the effect on the tropospheric temperature comes through the non-local scheme interacting better with the convection scheme (Gregory and Rowntree, 1990) which has a stability dependent closure for its initial mass flux. Timestep-by-timestep output (not shown) from a single column version of the unified model including the non-local turbulent mixing has a smoother evolution of convective activity.

Figure 12 shows a substantial difference in the contributions to the temperature increments in the boundary layer (zonally meaned for 50°N) from convection and turbulent mixing when the non-local scheme is used. (The "operational" zonally averaged increment profile is produced using the local mixing scheme and the "experimental" profile uses the non-local scheme.) The local scheme does not give large turbulent mixing increments in the boundary layer except in the bottom model layer. Heat is transported into this layer from the surface which the convection scheme then mixes upwards. The non-local scheme gives a more realistic balance between turbulent and convective increments in the boundary layer; there is no longer a cancellation of large increments at level 1. The convection scheme seems to almost switch off a turbulent mixing scheme based on fluxes calculated entirely in terms of *local* stability. The zonal mean of the profiles for all increments (dynamics and all physics) does not change substantially, just a small extra warming in model layers 1 and 2 when the non-local scheme is used.

Further evidence for the non-local scheme's effect on convection and low cloud simulation can be seen from a case study using the mesoscale version of the unified model. When the wind over Britain is from the north-west shower activity can be funnelled through the Cheshire gap into the Midlands region of England. Figures 13(a)

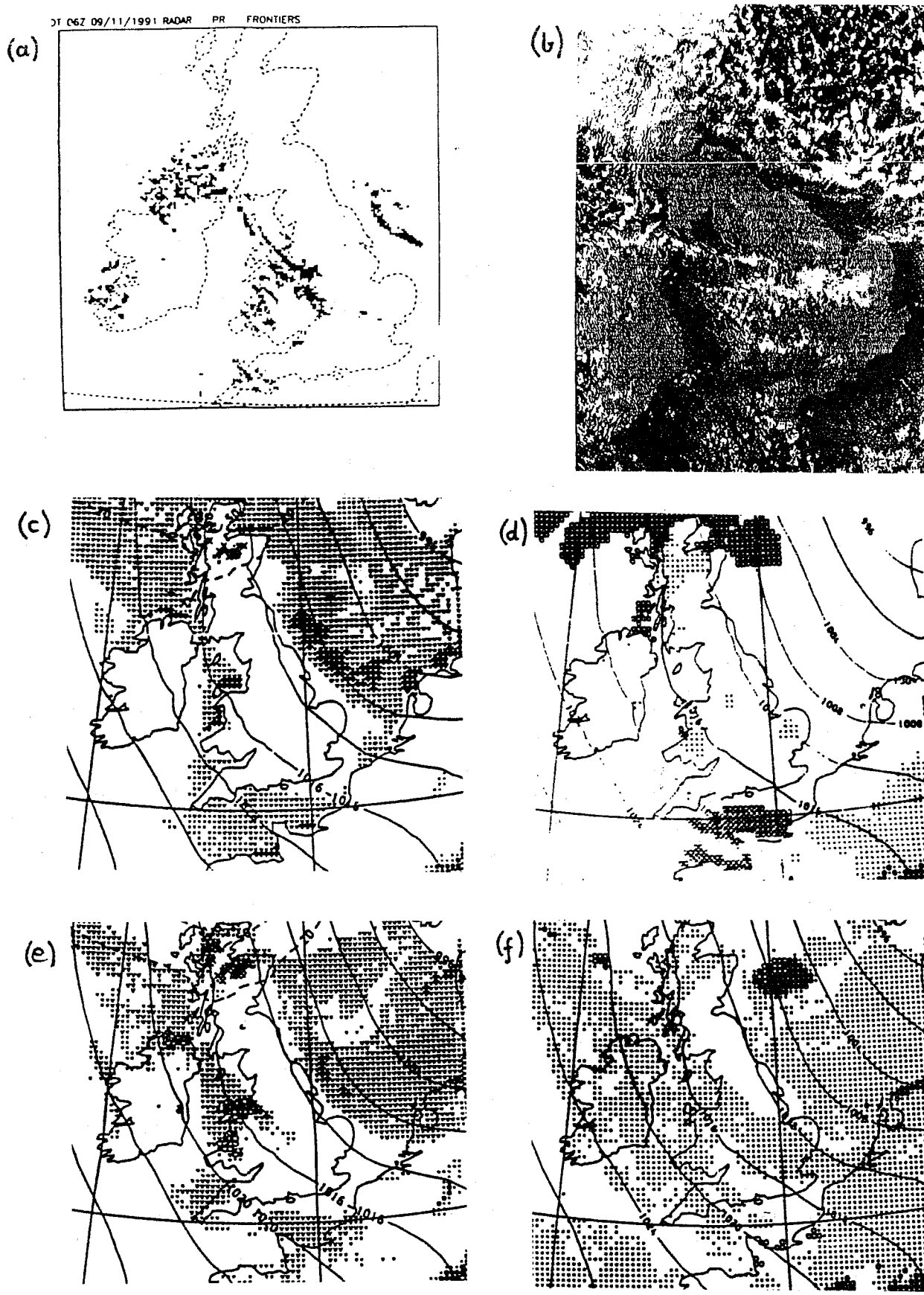

Figure 13. Case study for 9 November 1991 using the mesoscale model:
(a) Radar rainfall for 06Z, (b) Cloud from satellite at 04.30Z;
(c) T+24 precipitation forecast verifying at 06Z 9/11/91 from model with local turbulent mixing scheme, (d) same as (c) but showing forecast low and medium cloud; (e) and (f) as (c) and (d) respectively but from model with the non-local mixing scheme.

and 13(b) show such a situation on 9 November 1991at 06Z as seen by radar and satellite respectively. Figures 13(c) and 13(d) show the mesoscale model's T+24 forecast of precipitation and low cloud respectively for this time when the local mixing scheme was used. There is clearly little inland penetration of showers. When the non-local mixing scheme was put in the model a more satisfactory forecast was produced as can be seen from Figures 13(e) and 13(f).

4. Summary and conclusions

Recent changes to the large-scale cloud and precipitation schemes have improved the low cloud and albedo simulated in the climate version of the unified model. However, there is still too much cloud water in mid-latitudes and a marked deficiency in oceanic subtropical stratocumulus. It is not yet known whether the remaining errors are caused by the model's cloud scheme.

A modification to the way turbulent fluxes and increments are calculated helps alleviate the climate model's tropospheric temperature bias but had only a small effect on the simulated low cloud. The beneficial effect the non-local mixing scheme has on the initiation of convection is particularly interesting. This indicates that the way the model's turbulent mixing and convection schemes interact should be studied further.

Acknowledgements

I thank Cath Senior, Ruth Carnell and Andy Jones of the Climate Research Division of the UK Met Office; Sean Milton of the Forecasting Research Division and Sue Ballard of the Atmospheric Processes Research Division for allowing me to use results and producing diagrams from their model simulations and forecasts.

References

Greenwald,T.J., Stephens,G.L., Vonder Haar,T.H. and Jackson,D.L., 1993: A physical retrieval method of liquid water over the global oceans using SMM/I observations. *J. Geophys. Res.* (in the press).

Gregory,D. and Rowntree,P.R., 1990: A mass flux convection scheme with representation of cloud ensemble characteristics and stability dependent closure. *Mon. Wea. Rev.* **118**, 1483-1506.

Ingram,W.J., 1993: Unified Model Documentation Paper No. 23: Radiation. (Available from the Unified Model Librarian, Forecasting Research Division, Meteorological Office, London Road, Bracknell, Berkshire, RG12 2SZ, UK)

Smith,R.N.B., 1990: A scheme for predicting layer clouds and their water contents in a general circulation model. *Quart. J. Roy. Meteorol. Soc.* **116**, 435-460.

Smith,R.N.B., 1993: Unified Model Documentation Paper No. 24: Subsurface, Surface and Boundary Layer Processes. (Available from the Unified Model Librarian, Forecasting Research Division, Meteorological Office, London Road, Bracknell, Berkshire, RG12 2SZ, UK)

Stull,R.B., 1984: Transilient turbulence theory, Part I: The concept of eddy mixing across finite distances. *J. Atmos. Sci.*, **41**, 3351-3367.